Molecular Crystals and Liquid Crystals
Publication details, including instructions for authors and subscription information:
http://www.tandfonline.com/loi/gmcl16

X-ray Photographic Studies of Liquid Crystals: III. Structure Determination of the Smectic Phase of 4-Butyloxybenzal- 4′-Ethylaniline

Adriaan de Vries [a] & Derry L. Fishel [b]

[a] Liquid Crystal Institute, Kent State University

[b] Liquid Crystal Institute and Chemistry Department, Kent State University, Kent, Ohio, 44242, U.S.A.

Version of record first published: 21 Mar 2007.

To cite this article: Adriaan de Vries & Derry L. Fishel (1972): X-ray Photographic Studies of Liquid Crystals: III. Structure Determination of the Smectic Phase of 4-Butyloxybenzal- 4′-Ethylaniline, Molecular Crystals and Liquid Crystals, 16:4, 311-332

To link to this article: http://dx.doi.org/10.1080/15421407208082794

Molecular Crystals and Liquid Crystals. 1972. Vol. 16, pp. 311–332
Copyright © 1972 Gordon and Breach Science Publishers
Printed in Great Britain

X-ray Photographic Studies of Liquid Crystals†

III. Structure Determination of the Smectic Phase of 4-Butyloxybenzal-4′-Ethylaniline

ADRIAAN DE VRIES

Liquid Crystal Institute
Kent State University

and

DERRY L. FISHEL

Liquid Crystal Institute and
Chemistry Department
Kent State University
Kent, Ohio 44242, U.S.A.

Received April 8, 1971

Abstract—A new type of smectic phase (smectic H) is described, using microscopic and X-ray data. The structure of this phase can be assigned a three-dimensional monoclinic lattice, with $a = 10.32$ Å, $b = 4.986$ Å, $c = 20.73$ Å, and $\beta = 123.8°$, probably space group $P2_1$ or Pa. The *ab* plane is parallel to the smectic layers; the thickness of the layers is 17.27 Å. The molecules are most probably approximately parallel to the *c* axis, thus making an angle of 56.2° with the smectic layers and forming continuous columns of molecules parallel to the *c* axis. In planes perpendicular to the *c* axis the arrangement of the molecular axes is approximately hexagonal, with a spacing of 4.97 Å. Successive layers of molecules parallel to the *bc* plane are shifted 2.87 Å with respect to each other in the direction of the *c* axis. The most probable arrangement of the molecular planes is a herringbone-type packing. It appears that within the regular three-dimensional structure there are a considerable number of columns of molecules displaced parallel to the *c*-axis, thus giving rise to continuous diffuse planes in the reciprocal lattice.

1. General Introduction

The compound dealt with in this paper, 4-butyloxybenzal-4′-ethylaniline (BEA for short), $C_4H_9O \cdot C_6H_4 \cdot CH:N \cdot C_6H_4 \cdot C_2H_5$,

---

† Research supported by the Air Force Office of Scientific Research under Contract F44620-69-C-0021.

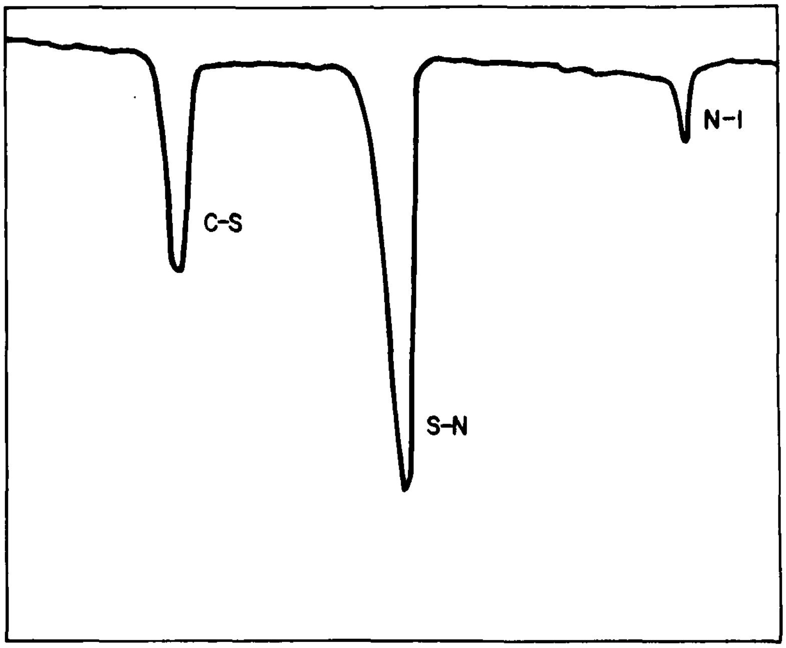

Figure 1. DTA thermogram; heating rate 5 °/min, sample size 5 mg. The temperature is plotted along the horizontal axis, Δt along the vertical axis.

first drew our attention because of its unusual DTA (differential thermal analysis) diagram (Fig. 1): the heat of transition of the S–N transition was larger than for the C–S transition, whereas usually the last one is by far the largest one. It was decided, therefore, to make an extensive investigation of this compound, using X-ray diffraction and microscopic studies.

The diffraction pattern obtained from the smectic phase of BEA turned out to be very unusual indeed; as far as we know, no similar patterns have been reported in the literature. The data presented in this paper show that we are dealing here with a smectic phase with an unusually high degree of order, in fact, three-dimensional order. It would, therefore, be legitimate to ask whether this particular phase of BEA is indeed a smectic phase or whether it more properly should be called a crystalline phase. We feel that the evidence from microscopic studies presented in this paper establishes definitely that the phase under study should be classified as a smectic phase.

2. Preparation and Purity

The compound was prepared by condensing 4-*n*-butyloxybenzaldehyde with 4-ethylaniline in absolute ethanol. The anil was recrystallized from ethanol and dried over calcium chloride in a vacuum desiccator. A mass spectrum shows ions at m/e 281 ($M^{+\cdot}$), 266, 225, and 210 as major contributors to the fragmentation pattern. No evidence for contamination of the sample with higher or lower homologues in the series of anils was found.

3. DTA Results

A freshly purified (recrystallized from ethanol) sample of 4-*n*-butyloxybenzal-4′-ethylaniline produced the DTA thermogram† (heating mode) illustrated in Fig. 1. Corrected transition temperatures (± 0.5°, all involving endothermic changes on heating) obtained by this method are 40.5° for the C–S point, 51° for the S–N point and 65.5° for the N–I point. Although accurate transition enthalpies cannot be extracted from these data, it is possible to obtain estimates of these enthalpies from the areas under the corresponding peaks in the DTA curve. It can be seen that the second transition involves the largest enthalpic change, consistent with the greatest alteration in ordering for the three transitions.

4. Microscopic Studies

As will be seen later on in this paper, the results from the X-ray diffraction work indicate a rather pronounced " crystalline " character for the " smectic " phase of BEA, and for this reason in our microscopic studies particular attention was given to those effects which would enable us to decide whether this particular phase should be classified as solid or as smectic.

A thin-section sample prepared for observation with a polarizing microscope (Reichert Thermopan) shows obvious changes in morphology at 41° (analogous to melting), 51° (transition to nematic phase) and 65° (clearing to isotropic liquid) by heating. When the same sample is slowly cooled from the isotropic melt, a marbled

---

† Obtained with a DuPont DTA 920.

texture appears at 66°; cover slip pressure produces the light flashes and threaded appearance typical of the nematic phase. At 52° straight elongated blade-like structures grow in (Fig. 2) and quickly develop discontinuities which result in a gross mosaic texture by the time the transition is completed (Fig. 3). This texture† is stable until the sample is cooled to 36° when a slow change in morphology to a prismatic crystalline phase occurs. The mosaic texture is maintained for several hours if the sample is cooled rapidly (without disturbance) to room temperature. There is a resistance to cover slip displacement and a tendency for the cover slip to break loose if pressure is abrupt; this phase can, however, be made to flow although it is quite viscous. If displacement is attempted at the temperature of transition (52–53°) a bi-refringent globular texture appears.

Although this substance shows morphologic changes most like the smectic B of Sackmann and Demus there is no true " fan-shape " texture intermediate between the nematic and the smectic mosaic textures.

These observations present convincing evidence that the phase under consideration is a smectic and not a solid phase :‡

(1) There is no supercooling at the transition from the nematic phase, whereas most N–C transitions show considerable supercooling.
(2) A change like that from Fig. 2 to Fig. 3 is not expected during the crystallization of a solid phase.
(3) The texture of the phase (Fig. 3) resembles that of a smectic B phase, not that of a solid phase.
(4) The phase can be made to flow.

5. X-ray Diffraction Results

Samples of BEA were prepared in glass capillaries of 0.5 mm diameter, and X-ray diffraction patterns (using Ni-filtered Cu radiation)

---

† Individual " blocks " in the mosaic texture here are larger in size than those reported by Sackmann and Demus(1) for smectic B mesophases.

‡ This conclusion is further supported by the results of a comparative study of the smectic phases of BEA and a number of its higher homologues.(2)

Figure 2. The smectic phase as it starts appearing in the nematic phase upon cooling. Temperature at the S–N point; magnification 100 × .

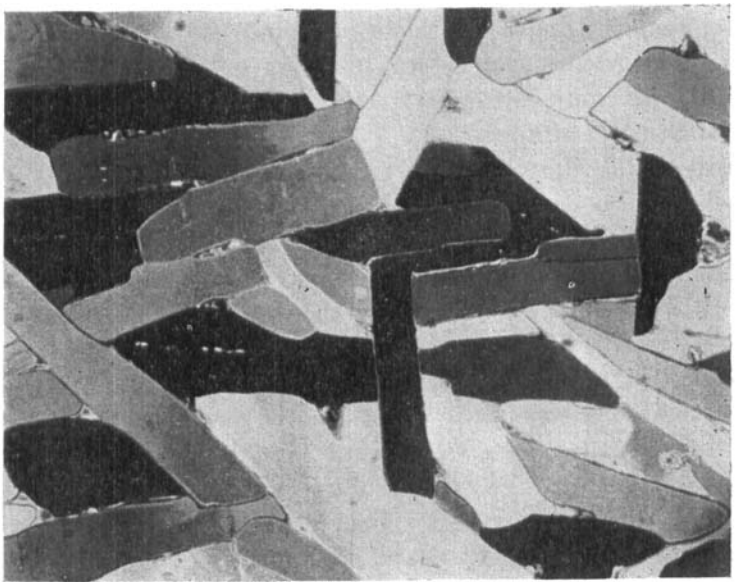

Figure 3. The smectic phase after the transition from the nematic phase is completed. Temperature about 48 °C; magnification 100 × .

were recorded on flat film with the set-up described earlier.(3) Preliminary studies indicated that the diffraction patterns contained not only many sharp reflections in an apparently hexagonal arrangement, but also continuous diffuse lines. To facilitate interpretation of the photographs, it was decided to try to obtain a smectic single crystal by aligning the molecules in a magnetic field.

With the film holder, the collimator and the collimator support removed, and by moving the camera somewhat away from the X-ray tube, it was possible to bring a permanent magnet around the sample in such a way that the direction of the magnetic field was approximately parallel to the direction of the incident X-ray beam (in the reassembled camera) and thus approximately perpendicular to the direction of the capillary axis. The field strength at the sample was about 1500 gauss. With the magnet in place, several attempts were made to align the sample by heating it first to the nematic phase and then cooling it to the smectic phase; this process was repeated two to four times. Although the resulting structure was much more uniform than that obtained by simply melting the solid (without magnetic field), we did not obtain a satisfactorily well aligned sample. The sample was then heated to the isotropic phase (68 °C) and subsequently cooled to the smectic phase (44.6°), in the magnetic field. The resulting structure, although not yet a perfect single crystal, was quite satisfactory, and all data reported here are obtained from this sample.

Keeping the sample at 44.6 °C, a large number of Polaroid photographs and some regular negatives were obtained, while rotating the capillary around its axis a few degrees at a time between photographs, but keeping the capillary always in a constant position during the photographs. Figure 4 shows the diffraction pattern obtained with the capillary in the position which it occupied during the cooling process (we shall define this position as $\phi = 0°$). The general hexagonal symmetry of the pattern can be seen, even though not all the equivalent maxima are present. Figure 5 shows the diffraction pattern obtained after a rotation of the capillary of 90° ($\phi = 90°$). In addition to some sharp and diffuse maxima (identified in Fig. 5b), one observes the first and second orders of continuous lines on each side of the center. On other photographs we were able to distinguish up to the fifth order of these lines.

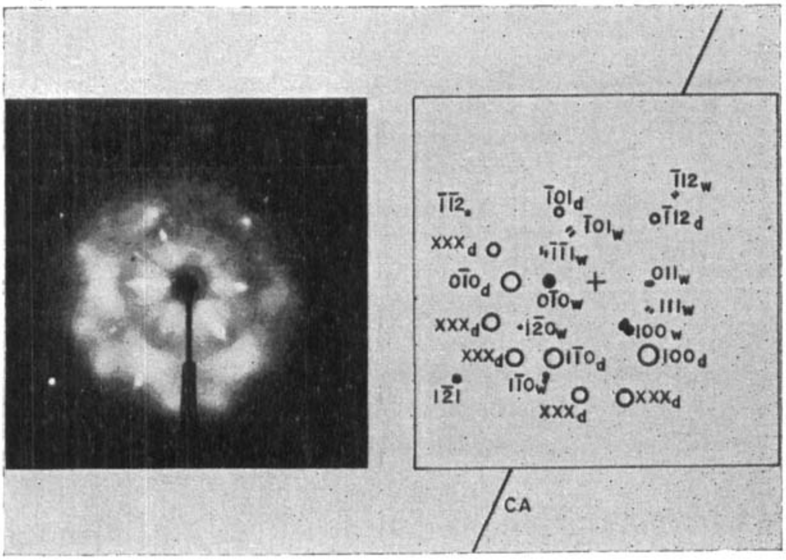

Figure 4. Diffraction pattern with the molecules approximately parallel to the incident beam ($\phi = 0°$). The double spots indicate that the sample was not a perfect single crystal. *a*: Actual photograph. *b*: Schematic diagram, identifying the reflections and the direction of the capillary axis (CA); the subscript *d* identifies a diffuse reflection (these are represented by the open circles), the subscript *w* a sharp reflection caused by white radiation, and the absence of a subscript means that the reflection is caused by Cu K α radiation; the center of the film is indicated by a + sign.

A further examination of all the photographs indicated that the reciprocal lattice consisted of a set of parallel planes, each plane containing a hexagonal array of sharp lattice points, each point being surrounded by a diffuse region. These reciprocal lattice planes, moreover, coincided with continuous diffuse planes (which cause the continuous diffuse lines as seen on Fig. 5), except that there was no continuous diffuse plane through the center of the reciprocal lattice.

6. Introduction to Discussion of X-ray Data

The discussion of the X-ray results will consist mainly of an analysis of the data obtained from the sharp reflections. This analysis can be divided into three parts. First, the unit-cell parameters of the three-dimensional lattice are derived from the measurements in a fairly straightforward way (sections "Assignment of

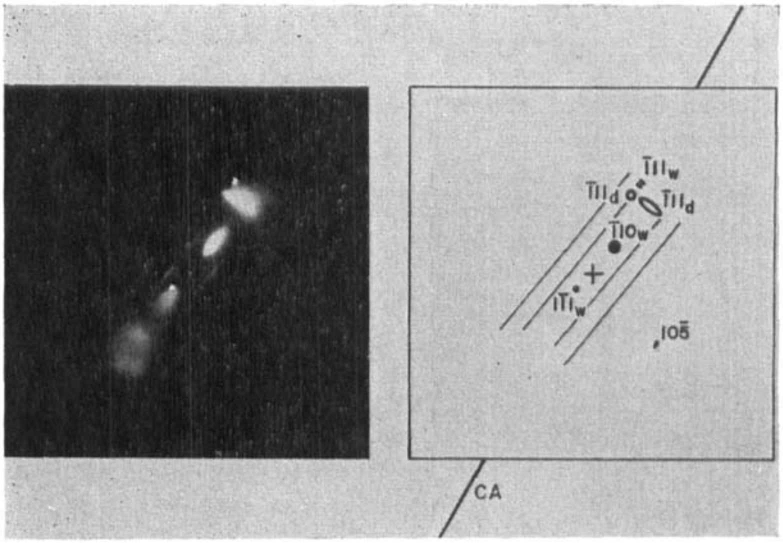

Figure 5. Diffraction pattern with the molecules perpendicular to the incident beam ($\phi = 90°$). *a*: Actual photograph. *b*: Schematic diagram.

Reciprocal Lattice " and " Cell Parameters for Reciprocal and Real Lattice "). Second, the direction of the long molecular axis with respect to the lattice is determined; this is a much less straightforward process and it involves some speculation, but the final conclusion may still be considered fairly certain (" Model of the Structure "). Third, a model is presented for the most probable orientations of the molecular planes; here there is less certainty about the correctness of the conclusions reached (" Orientation of the Molecular Planes ").

The diffuse diffraction phenomena are discussed briefly in the section on " Diffuse Diffraction Effects ". The most important of these effects are the continuous diffuse diffraction lines, and the interpretation of these lines plays also an important role in the section on " Model of the Structure ".

7. Assignment of Reciprocal Lattice

A careful study of the photographs enabled us to index a large number of reflections on the basis of a three-dimensional reciprocal lattice consisting of the sharp lattice points. The correctness of this interpretation of the diffraction pattern is attested to by the close agreement between measured values of the distances of the reflections from the center of the film, and the values calculated on the basis of the reciprocal lattice (Table 1, columns 2 and 3). We want to emphasize here in particular that the *three-dimensional* character of the lattice is established beyond doubt by several reflections of fairly high order in l.

The reciprocal lattice was defined in such a way that the a^* and b^* axes lie in the reciprocal lattice planes mentioned above (with a hexagonal arrangement of the lattice points); thus all points in such a plane have the same index l. One of these lattice planes is shown in Fig. 6. Although we have not been able to detect significant deviations from the hexagonal symmetry within each plane, the overall symmetry of the lattice can not be hexagonal since the planes

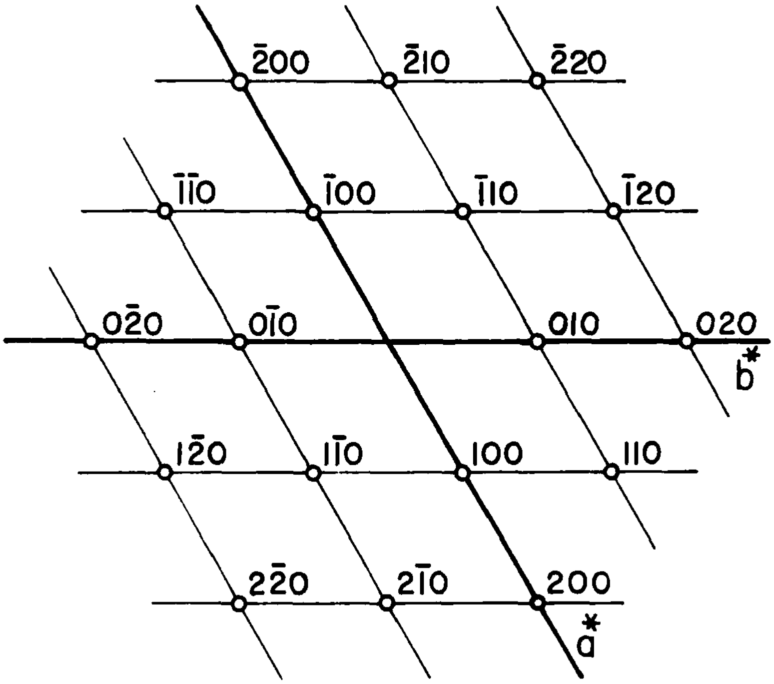

Figure 6. The a^*b^* plane of the reciprocal lattice, oriented so as to correspond with Fig. 4.

TABLE 1 Measured and Calculated Reflection Positions

$(hkl)_{ph}$	r_m	r_{c_1}	r_{c_2}	$(hlk)_m$
001	4.4	4.5	4.5	001
2	9.2	9.1	9.2	2
3	14.0	13.9	14.0	3
4	18.8	19.0	19.0	4
5	24.5	24.4	24.5	5
$01\bar{4}$	23.3	23.5	23.4	$11\bar{4}$
$\bar{3}$	21.1	20.6	20.5	$\bar{3}$
$\bar{2}$	18.5	18.8	18.7	$\bar{2}$
$\bar{1}$	18.0	18.2	18.2	$\bar{1}$
0	19.0	19.0	19.0	0
1	21.3	21.1	21.1	1
$1\bar{2}\bar{1}$	37.7	37.5	37.3	$0\bar{2}\bar{1}$
0	37.1	36.9	36.8	0
1	37.0	37.5	37.3	1
$1\bar{1}\bar{3}$	20.3	20.6	20.5	$1\bar{1}\bar{3}$
$\bar{2}$	18.9	18.8	18.7	$\bar{2}$
$\bar{1}$	18.3	18.2	18.2	$\bar{1}$
0	19.0	19.0	19.0	0
1	21.2	21.1	21.1	1
2	24.0	24.1	24.2	2
3	28.9	28.2	28.2	3
4	33.2	33.1	33.2	4
$10\bar{5}$	20.7	21.0	20.8	$20\bar{5}$
$\bar{4}$	17.8	18.0	17.9	$\bar{4}$
$\bar{3}$	16.2	16.2	16.1	$\bar{3}$
$\bar{2}$	15.9	15.7	15.7	$\bar{2}$
$\bar{1}$	17.0	16.7	16.7	$\bar{1}$
0	19.2	19.0	19.1	0
1	22.1	22.4	22.5	1
$11\bar{2}$	31.8	32.1	32.1	$31\bar{2}$
$\bar{1}$	34.2	34.0	34.0	$\bar{1}$
0	—	36.9	37.0	0
1	41.1	40.9	41.1	1
$2\bar{1}\bar{2}$	31.8	32.1	32.1	$3\bar{1}\bar{2}$
$\bar{1}$	34.0	34.0	34.0	$\bar{1}$
0	37.1	36.9	37.0	0
1	40.8	40.9	41.1	1
$20\bar{4}$	34.8	35.3	35.2	$40\bar{4}$
$\bar{3}$	36.5	36.3	36.2	$\bar{3}$
$\bar{2}$	—	38.3	38.3	$\bar{2}$
$\bar{1}$	41.5	41.3	41.4	$\bar{1}$
0	46.0	45.5	45.7	0

$(hkl)_{ph}$ and $(hkl)_m$ are the reflection indices based on the original pseudo-hexagonal (triclinic) and the final monoclinic reciprocal lattice, respectively; r_m, r_{c_1} and r_{c_2} are the distances from the center of the reflection to the center of the film, measured, calculated for the triclinic lattice, and calculated for the monoclinic lattice, respectively (all for Cu K_α radiation). Values for $\overline{hkl}$ reflections (when measured) are included under the corresponding hkl listing.

are shifted with respect to each other and the c^* axis is thus not perpendicular to the a^*b^* plane. The projection of the c^* axis on the a^*b^* plane was found to be 29.2° away (clockwise in Fig. 6) from the ***hho*** direction, and therefore only 0.8° from the a^* axis. Since this was well within the error of the measurement, we have assumed for all our calculations that the projection of the c^* axis coincides exactly with the a^* axis (the conclusions reached further on in this paper are not significantly influenced by this assumption). Thus the a^*c^* plane, shown in Fig. 7, is perpendicular to the a^*b^* plane; the angle between the a^* and c^* axes was calculated as 56.80°.

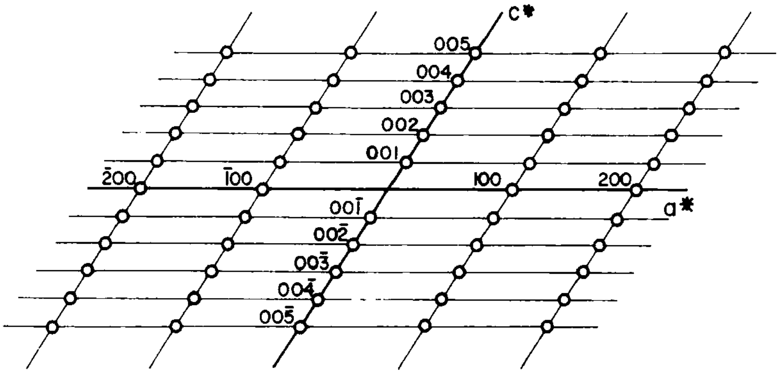

Figure. 7 The a^*c^* plane of the reciprocal lattice.

8. Cell Parameters for Reciprocal and Real Lattice

The values obtained for the unit-cell parameters† of the reciprocal lattice described above are as follows: $a^* = b^* = 4.305$ Å (with a standard deviation σ estimated at 0.01 Å), $c^* = 17.27$ Å ($\sigma \approx 0.02$), $\alpha^* = 74.1°$, $\beta^* = 56.8°$ and $\gamma^* = 60.0°$ (for the angles $\sigma \approx 0.3°$).

From these values the unit-cell parameters of the real-space lattice can be calculated as follows: $a = 5.71$ Å, $b = 4.97$ Å, $c = 20.64$ Å, $\alpha = 90.0°$, $\beta = 119.5°$ and $\gamma = 115.8°$. This lattice is triclinic.

It is also possible, though, to choose the reciprocal axes differently: a^* could be taken in the same direction as before, but with half the

---

† These unit-cell parameters were calculated on the basis of the distances of the reflections from the center of the film, the angular positions of the reflections, and the angular positions of the capillary.

original spacing, b^* could be taken perpendicular to a^* (in the old $\bar{1}20$ direction; see Fig. 6), with a spacing of 0.8660 ($= \cos 30°$) times the original spacing, and c^* could be kept the same. This set of axes would give the same lattice points as the original reciprocal lattice, plus another set halfway between the original points on lines parallel to the a^* axis. Since the reflections corresponding to this second set of lattice points have not been observed, there would have to be extinction conditions prohibiting these extra reflections. Retaining the assumption that the projection of c^* on the a^*b^* plane falls exactly along a^*, the new reciprocal lattice has the b^* axis perpendicular to both the a^* and the c^* axes, and thus is monoclinic.

The corresponding real-space lattice has as parameters: $a = 10.29\,\text{Å}$, $b = 4.97\,\text{Å}$, $c = 20.64\,\text{Å}$, $\beta = 123.2°$, ($\alpha = \gamma = 90°$). In order to provide the necessary extinction conditions referred to above, the lattice would have to be centered in the ab plane. This monoclinic C lattice would give exactly the same diffraction pattern as the triclinic lattice defined earlier, but the model of the structure, to be discussed below, corresponds more naturally to the monoclinic lattice, and for this reason we prefer the monoclinic representation.† To test the agreement between the measured reflection positions and the monoclinic symmetry, we indexed all measured reflections (Table 1) on the basis of the monoclinic lattice and performed least-squares refinements of the unit-cell parameters on the basis of the r_m values, first keeping $\alpha = \gamma = 90°$ (i.e., imposing monoclinic symmetry) and next leaving α and γ free (i.e., allowing the lattice to refine as a triclinic lattice). The differences between the two calculations were so minimal (in particular, the triclinic lattice gave $\alpha = 90.3°$ and $\gamma = 89.9°$), that we feel justified in describing the structure in terms of a monoclinic lattice (although, of course, we have no *proof* that the lattice is monoclinic). The parameters obtained from the least-squares calculation for the monoclinic lattice are: $a = 10.32\,\text{Å}$ ($\sigma = 0.06$), $b = 4.986\,\text{Å}$ ($\sigma = 0.01$), $c = 20.73\,\text{Å}$ ($\sigma = 0.20$), $\beta = 123.8°$ ($\sigma = 0.2$). Reflection positions calculated from these parameters are given in Table 1 (r_{c_2} values). Projections of the monoclinic lattice along the c and b axes are given in Fig. 8. From Fig. 8a it can be

---

† For the sake of convenience we have retained, however, throughout the paper (except in the last column of Table 1), the reflection indices based on the original pseudo-hexagonal reciprocal lattice as represented in Figs. 6 and 7.

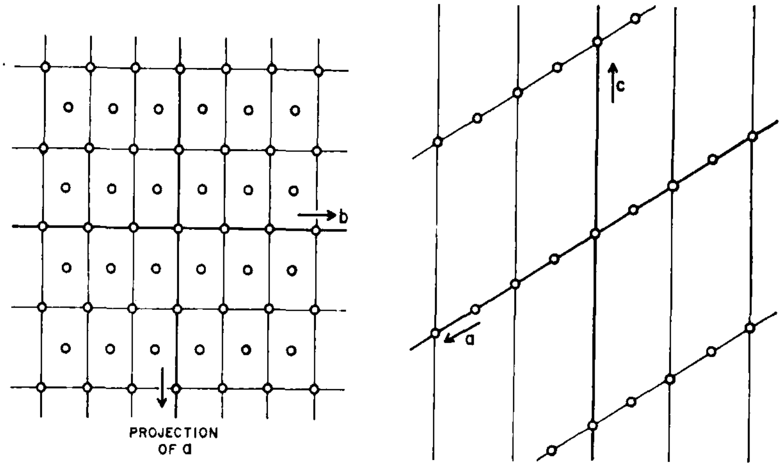

Figure 8. The real-space lattice. *a*: Projection along the *c*-axis. *b*: Projection along the *b*-axis.

seen that in the projection along the *c* axis the lattice points (the circles) form a hexagonal array (with a spacing of 4.97 Å),† corresponding to the one in the a^*b^* plane of the reciprocal lattice.

9. Diffuse Diffraction Effects

In addition to the sharp reflections corresponding to the points of the reciprocal lattice, the photographs also show diffuse maxima and diffuse lines. Most of the diffuse maxima can be identified as caused by diffuse areas in the reciprocal lattice surrounding the lattice points. They may thus be regarded as caused by thermal motion and disorder in the lattice.

There is one set of diffuse maxima (indicated by the indices xxx in Fig. 4b), located in the a^*b^* plane about halfway between the 100 and 110 reflections (see Fig. 6) and between similar pairs of reflections, for which no corresponding sharp reflections were observed. Their positions in the reciprocal lattice would correspond with the

---

† The unit-cell dimensions of this pseudo-hexagonal lattice are 4.986 Å along the *b* axis and 4.962 Å along the other two hexagonal axes. The angles between the *b* axis and these other two axes are 120.2°. Considering the standard deviations of the parameters, these deviations from hexagonal symmetry are not significant, and the average spacing is 4.970 Å.

positions of {120} reflections from a lattice with spacings twice as large as those of the triclinic lattice given above.

At this point we might mention too, that the diffuse {100} reflections give the rather strong impression of being the intersection of two broad diffuse streaks (see Fig. 4a). For the 100 reflection these streaks run parallel to the 010 and the $\bar{1}10$ directions, respectively (see Fig. 6); for the other {100} reflections the situation is analogous. We do not have a definite explanation yet for either of these two effects (the presence of the xxx maxima and the structure of the {100} reflections), but most probably they are caused by deviations from the regular packing of the molecules.

The continuous diffuse lines (as seen on Fig. 5a) indicate the presence of continuous diffuse planes in the reciprocal lattice, as discussed above (last paragraph of " X-ray Diffraction Results "). The lines are analogous to the continuous lines found in diffraction photographs obtained from fibers,$^{(4)}$ and they point to the existence of a real-space lattice with a regular periodicity in only one dimension (see, e.g., Fig. 2 in Ref. 5). The repeat period determined from the distance between the diffuse reciprocal lattice planes is 20.73 Å, and its direction is parallel to the c axis of the three-dimensional lattice (because the diffuse planes coincide with the three-dimensional lattice planes parallel to the a^*b^* plane). At first sight, the existence of a one-dimensional lattice would seem to be in conflict with the existence of a three-dimensional lattice as established above. We shall see presently, however, that both lattices can be explained by a single model for the molecular structure of this smectic phase.

10. Model of the Structure

The determination of the unit cell parameters was a fairly straightforward matter, but this is not the case for the derivation of a model for the molecular packing. The unit cell fixes only the positions of the *centers* of the molecules, and for a rigorous determination of the *orientation* of the molecules around these centers one would need the measured intensities of the various reflections, and these intensities cannot be obtained from our photographs. For the derivation of a model, therefore, we shall have to base ourselves more on plausible assumptions than on hard facts. Our main assumptions will always be well documented, however, and we feel quite confident that the model we shall develop here is a good approximation to the true structure.

We note first that the value of the unit cell parameter c (20.73 Å) is quite close to the length of an extended molecule of BEA calculated from a model(6) (21.5 Å). This indicates that the long axis of the molecule is parallel (or nearly so) to the direction of the c axis. The small difference between the two values can easily be explained by a slight " overlap " of the ends of the molecules (a similar explanation was offered for the difference between molecular length and the thickness of the smectic layer in smectic A phases(6)). If we would assume that the molecules were indeed parallel to the c axis, then the arrangement of the molecular axes would be given by the arrangement of the lattice points as projected onto a plane perpendicular to the c axis. It was shown above (under " Cell Parameters for Reciprocal and Real Lattice ") that the arrangement in this plane is approximately hexagonal with a distance of 4.97 Å between the points; thus the intermolecular distance would also be 4.97 Å. This value is very close to the value of 4.89 Å found(6) for the intermolecular distance of a rather similar molecule (ethyl-*p*-ethoxybenzal-*p*-aminobenzoate, EEB for short) in the smectic A phase, and this gives additional support for the assumption that the molecules are parallel to the c axis. We shall therefore take this assumption as correct. The molecular packing which follows from this is shown in Fig. 9 using cylindrical molecules: in a plane perpendicular to the long axes the packing of the molecules is hexagonal, but successive layers of molecules (parallel to the bc plane) are displaced in the direction of the c axis over a distance of 2.87 Å.

There are three features of the model proposed above, that we wish to point out in particular. One is that the smectic layers are parallel to the ab plane, and that the molecules stand at an angle of 56.2° with respect to the planes of the smectic layers. Thus, the smectic phase is a " skewed smectic phase ", similar in this respect to the smectic C phase,(7,8) but with a much higher degree of order.

The second point to be stressed is that the existence of a three-dimensional lattice, incorporating a large number of smectic layers, shows that the mobility of the smectic layers with respect to each other is very limited in this phase (this is confirmed by the observed high viscosity).

The third point is that adjacent smectic layers appear to be positioned in such a way that the long axes of the molecules in each layer are collinear with the long axes of the molecules in the adjacent layers, thus creating continuous columns of molecules, in head-to-tail arrangement, in the direction of the *c* axis; the distance between the centers of neighboring molecules in these columns is 20.73 Å. As pointed out above, in the last paragraph of " Diffuse Diffraction Effects ", the continuous lines in the diffraction pattern indicate the existence of a one-dimensional structure with a repeat period of 20.73 Å parallel to the *c* axis of the three-dimensional lattice. The similarities between this one-dimensional structure and the columns of molecules just discussed are evident. We propose, therefore, that the observed continuous diffraction lines are caused by the displace-

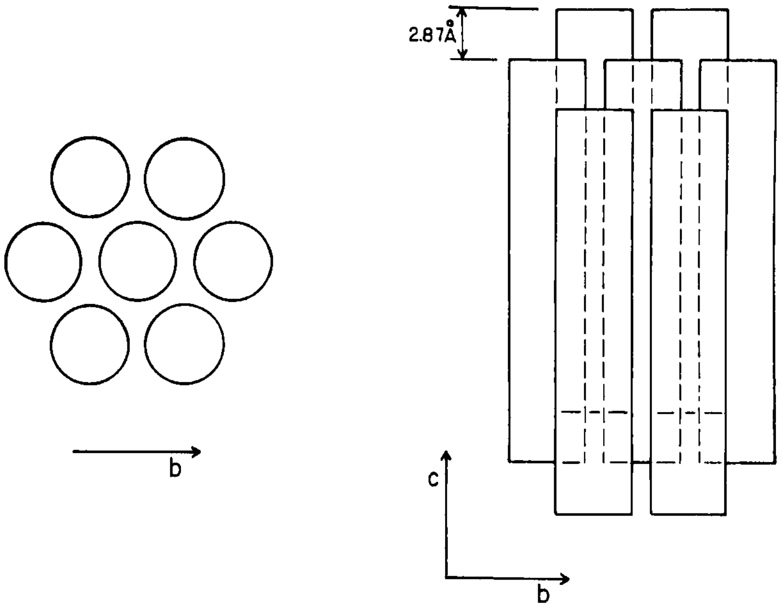

Figure 9. Packing of the molecules (for reasons of clarity the molecular diameter has been taken smaller than the intermolecular distance; actually, of course, the molecules are in contact with each other). *a*: View along the *c* axis. *b*: View perpendicular to the *bc* plane.

ment of several of these columns of molecules,† parallel to the c axis, out of their proper positions in the three-dimensional lattice, and with no regular relationship between the positions of the displaced columns (the majority of the columns remains in place, however, so that the overall three-dimensional order of the lattice is preserved). Such a displacement would produce exactly the diffraction pattern observed: continuous reciprocal lattice planes coincident with planes of the regular reciprocal lattice for $l = \pm 1, 2, 3$, etc., but no continuous plane for $l = 0$.

An interesting speculation can be made in connection with the second and third point discussed above. If the structure of the material was completely given by a regular three-dimensional lattice (implying a very limited mobility of the smectic layers), it would not be clear in what respect this structure would differ from a true crystal structure. The observation, however, that apparently a considerable number of molecules (in columns parallel to the c axis) have moved out of the smectic layers, offers a way out of this dilemma: it may be that the smectic layers are relatively free to move with respect to each other *as long as the molecules composing the layers remain within the layers*, but that the layers become " locked " into special positions by the molecules that move partly out of the layers into neighboring layers. It appears to us that this hypothesis offers an explanation for the smectic rather than crystalline character of the phase (demonstrated by the microscopic studies), notwithstanding the presence of a three-dimensional lattice (demonstrated by the X-ray reflections).

From all these considerations a picture emerges of a structure with a very curious ambivalent character, a real " mesomorphic " structure! From the observations discussed in the section on " Microscopic Studies " it follows that we are dealing with a liquid crystalline phase, but the three-dimensional lattice structure implies a certain " crystalline " character. Then, the arrangement of the molecules in layers indicates that the structure is of a smectic

---

† It should be emphasized here that the existence of these columns depends upon our earlier conclusion that the long molecular axes are approximately parallel to the c axis. We consider this conclusion supported by the fact that these columns allow such a natural explanation of the continuous diffraction lines.

type, but the apparent mobility (in a limited way) of the molecules in the direction of their long axes suggests a certain " nematic " character. Thus, we find in one structure at the same time crystalline, smectic and nematic characteristics.

11. Orientation of the Molecular Planes

It was pointed out elsewhere(6) that the intermolecular distance in the smectic phase of EEB was too short to allow free rotation of the molecules around their long axes. This holds also for the smectic phase of BEA: the intermolecular distance is 4.97 Å, the width of a benzene ring is 6.7 Å. The regular, three-dimensional space lattice further points to a very orderly arrangement of the molecules. We have tried several different models, but the only satisfactory one appears to be a herringbone-type packing similar to that proposed by Gulrich and Brown.(9) Figure 10 shows a packing of this type with a hexagonal arrangement of the molecular axes.† It will be seen from this figure that in this type of packing the original three hexagonal axes (which make angles of 120° with each other, see Fig. 9a) are no longer all equivalent, although the spacings (between the molecular axes) in the three directions are still equal. The horizontal hexagonal axis in Fig. 10 differs from the other two

---

† A comparison of Figs. 10 and 8a shows that the herringbone structure automatically leads to a monoclinic lattice; hence our preference for the monoclinic description of the lattice over the triclinic one. The hexagonal arrangement of the molecular axes is achieved, however, for only one particular angle between the molecular planes and the *b* axis, and it may be expected that accurate measurements will reveal deviations from this hexagonal arrangement (see also the footnote on p. 323). For this reason we have used the terms " pseudo-hexagonal " and " approximately hexagonal ".

A comparison of Figs. 10 and 8a shows further that the lattice of the herringbone structure is no longer centered in the *ab* plane. With centrosymmetric molecules the space group would probably be $P2_1/a$, without a center $P2_1$ or Pa would be most likely. Thus the " additional reflections ", mentioned in " Cell Parameters for Reciprocal and Real Lattice ", would not all be zero any more. It may be expected, though, that they would be weak and so it is not surprising that we have not found these reflections in our study of the X-ray photographs. An interesting point is that four of these additional reflections would correspond in position with four of the diffuse {xxx} reflections (see Fig. 4) which we were unable to identify (see " Diffuse Diffraction Effects "); we have never observed any sharp reflections corresponding to those diffuse spots, though.

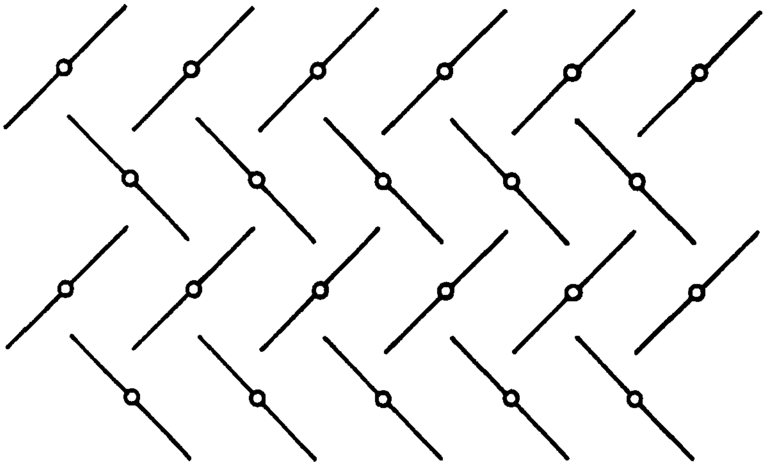

Figure 10. Schematic representation of a herringbone-type packing, as seen along the long axes of the molecules. The lines represent the directions of the planes of the molecules, the circles indicate the positions of the long axes of the molecules, which occupy the lattice points of a hexagonal lattice.

in that successive molecules along this axis all have the same orientation, whereas along the other two axes successive molecules alternate in orientation. When we compare this with the model of the structure shown in Fig. 9b, we see that here, too, one of the three hexagonal axes is different from the other two: along the *b* axis all molecules are on the same level whereas in the directions of the other two axes adjacent molecules are displaced in the direction of the *c* axis. Thus, if we accept the herring-bone-type packing as correct, it would be logical to identify the horizontal axis in Fig. 10 with the *b* axis of our structure; in each layer of molecules parallel to the *bc* plane all molecules would have the same orientation,† and successive layers (shifted along the *c*-direction) would alternate in molecular orientation. These conclusions, although their basis is admittedly rather weak, are given considerable support by data

---

† Strictly speaking, this would only have to be the case for "strips" of molecules in the *bc* plane with the same *c* parameter; adjacent strips could have different molecular orientation. This would make it very difficult, however, for columns of molecules parallel to the *c*-axis to move away from their lattice positions (as discussed at the end of the section on a "Model of the Structure"). We consider it more likely, therefore, that *all* molecules in a plane parallel to the *bc* plane have the same orientation.

obtained from a study of the molecular packing in the crystal structures of some aromatic compounds. In the structures of anthracene,(10) azobenzene,(11) biphenyl,(12,13) and naphthalene(14) we find exactly the same situation. All these structures contain layers of molecules which have their planes parallel to each other, and in these layers the molecules show only very small shifts with respect to each other in the direction of their long axes (just as in the layers along the *b* axis in Fig. 9b). Successive layers of this kind have alternating directions of the molecular planes (just as in Fig. 10) and are displaced significantly with respect to each other in the direction of the long axes of the molecules (just as in Fig. 9b). We feel, therefore, that we have sufficient reason to believe that Figs. 9b and 10 give the most probable molecular arrangement in the structure of the smectic phase of BEA.

12. Summary

We have presented data showing the existence of a new thermotropic smectic phase, quite unlike any of the ones that have been described before. The arrangement of the *centers* of the molecules could be determined accurately, but from the data at hand the *orientations* of the molecules could not be established with certainty. Based on various considerations, however, it was possible to develop a model for the packing of the molecules which may be considered a good approximation to the true structure.

The molecules are arranged in layers as in any smectic phase. They are inclined to the planes of the layers as in the smectic C phase, but show a much more ordered arrangement of the molecules within the layers. Moreover, neighboring layers are not free to slide over each other, as is usually the case for smectic phases, but are arranged in such a way that the centers of the molecules in a set of layers form a regular three-dimensional lattice with the *a* and *b* axes lying in the smectic layer and the *c* axis making an angle of 56.2° with the smectic planes (the *c* spacing is 20.73 Å, approximately equal to the length of the molecule, 21.5 Å). The molecules are probably close to being parallel to the *c* axis, and in a plane perpendicular to the *c* axis the arrangement of the *molecular axes* is approximately hexagonal, with a spacing of 4.97 Å. The *molecules* are most probably arranged in a herringbone-type packing, with successive layers of parallel molecules shifted 2.87 Å with respect to each other in the direction of their long axes. The space group would most likely be $P2_1$ or Pa. Within this regular three-dimensional structure there are a considerable number of columns of molecules displaced parallel to the *c* axis. The hypothesis is advanced that these columns of displaced molecules are essential rather than incidental to the structure of this phase, i.e., that the regular arrangement of neighboring smectic planes is actually caused by the displaced molecules.

In keeping with the classification scheme introduced by Sackmann and his colleagues, a new letter symbol will have to be assigned to this phase. The letters A, B, C, D and E have already been assigned to various smectic phases,(15) and just recently two new smectic phases have been given the letters F and G.(16) We would like to suggest the letter H for the type of smectic phase exhibited by BEA ;† the letter H seems a very appropriate symbol since the H can be taken to stand for " hexagonal ", in recognition of the apparent hexagonal character of the diffraction pattern of this phase.

This new smectic H phase is truly remarkable in several ways. It is, to our knowledge, the only thermotropic smectic phase for which a three-dimensional space lattice has been described in detail. It provides, therefore, a link between the other smectic phases and the crystalline phase. On the other hand, the apparent mobility (though limited) of the molecules in the direction of their long axes, gives the phase a certain " nematic " character.

Since this smectic H phase is such a remarkable one, it certainly warrants further study. We hope, therefore, in the near future to undertake a precise structure determination of this phase, using a single crystal diffractometer.

---

† After this paper was submitted for publication, an article came to our attention(17) which describes a smectic phase of terephthal-bis-(4-*n*-butylaniline). The diffraction patterns of this phase appear to be virtually identical with those discussed here.(18) Although this phase was classified as a smectic B phase, we prefer to use the name " smectic H " for phases of the type described in this paper (which may be considered skewed smectic B phases), and to reserve the designation " smectic B " for phases in which the molecules stand normal to the smectic planes. This proposed distinction between S_B and S_H phases is analogous to the commonly accepted one between S_A and S_C phases.

Acknowledgements

The authors express their appreciation to Dr. J. T. S. Andrews, who zone-refined the sample used for the collection of the X-ray data, to Dr. P. R. Patel, for his assistance with the microscopic studies, and to Miss Mary Ann Flandera, who assisted in the synthetic work and who is to be credited for making the photographs reproduced in Figs. 2 and 3.

REFERENCES

1. Sackmann, H. and Demus, D., *Mol. Cryst.* **2**, 81 (1966).
2. Fishel, D. F. and de Vries, A., to be published.
3. de Vries, A., *Mol. Cryst. and Liq. Cryst.* **10**, 219 (1970).
4. Warren, B. E., *Z. Krist.* **76**, 209 (1930).
5. Mabis, A. J., *Acta Cryst.* **15**, 1152 (1962).
6. de Vries, A., *Mol. Cryst. and Liq. Cryst.* **11**, 361 (1970).
7. Chistyakov, I. G., Schabischev, L. S., Jarenov, R. I. and Gusakova, L. A., *Mol. Cryst. and Liq. Cryst.* **7**, 279 (1969).
8. de Vries, A., *Acta Cryst.* **A25**, S135 (1969).
9. Gulrich, L. W. and Brown, G. H., *Mol. Cryst.* **3**, 493 (1968).
10. Cruickshank, D. W. J., *Acta Cryst.* **9**, 915 (1956).
11. Brown, C. J., *Acta Cryst.* **21**, 146 (1966).
12. Trotter, J., *Acta Cryst.* **14**, 1135 (1961).
13. Hargreaves, A. and Rizvi, S. H., *Acta Cryst.* **15**, 365 (1962).
14. Abrahams, S. C., Robertson, J. M. and White, J. G., *Acta Cryst.* **2**, 238 (1949).
15. Sackmann, H. and Demus, D., *Fortschr. Chem. Forsch.* **12**, 349 (1969).
16. Demus, D., Diele, S., Klapperstück, M., Link, V. and Zaschke, H., *Mol. Cryst. and Liq. Cryst.* in press.
17. Levelut, A. M. and Lambert, M., *C.R. Acad. Sci.* (*Paris*) **272B**, 1018 (1971).
18. Levelut, A. M., private communication.